Joint iterative migration of surface and borehole gravity gradiometry data

Le Wan[1,2], Muran Han[1], and Michael S. Zhdanov[1,2]*
[1]University of Utah, and [2]TechnoImaging

Summary

Gravity and gravity gradiometry surveys have been widely used in mineral and petroleum exploration. Borehole gravity measurements can help to detect a deep target, which is of importance in studying both mineral and hydrocarbon (HC) deposits. Joint interpretation of surface and borehole gravity data can provide more insight about the subsurface geological structures than separate surface and borehole data. The major goal of this joint interpretation is to produce a 3D density distribution under the area of the a surface survey and in the vicinity of a borehole. This paper develops a novel approach to solving this problem based on the concept of potential field migration, which produces images of the subsurface density distribution. By applying the migration iteratively, we can generate a rigorous inverse model of the density distribution. The method is illustrated by the joint migration of the borehole and surface data for a set of representative density models.

Introduction

Gravity gradiometry has become widely used in geophysical exploration since it can provide an independent measurement of subsurface density distribution. The advantage of gravity gradiometry over other gravity methods is that the data are extremely sensitive to local density anomalies within regional geological formations (Wan and Zhdanov, 2008). The high-quality data can be acquired from either airborne, ground, or marine platforms over very large areas for relatively low cost.

However, the sensitivity of the gravity field is inverse proportional to the square of the distance. Making use of borehole gravity measurements can significantly improve the inversion result. Borehole gravity measurements were pioneered by Smith (1950) and then applied to problems of reservoir evaluation by McCulloh et al. (1968). Unlike the shallower-sensing density log, the borehole gravimeter is insensitive to wellbore conditions such as rugosity and the presence of casing. The first-generation BHGMs (Borehole Gravity Meters) were limited to large-diameter, near-vertical boreholes and were deployed in wells for hydrocarbon (HC) exploration. The second-generation BHGM has been developed for mining and geotechnical applications (Nind et al. 2007; 2013). Prototype borehole gravity gradiometers have since been developed by Gravitec (e.g., Golden et al., 2007) and Lockheed Martin (DiFrancesco, 2007).

Several researchers have suggested to making joint use of the borehole and the surface data to improve the results of interpretation (e.g., Cao et al., 2013) and helping to overcome the narrower frequency bandwidth of the surface seismic data. Li and Oldenburg (2000) used 3D inversion of the surface and borehole magnetic data jointly to better define the deep target. Krahenbuhl and Li (2008) and Sun and Li (2010) conducted a feasibility study of the joint inversion of the surface and borehole gravity data. Also, Rim and Li (2010) and Liu and Zhdanov (2011) demonstrated the capability of interpretation the gravity and gravity gradiometry data from a single borehole.

In this paper we introduce a novel approach to the joint interpretation of the surface and borehole gravity data based on the concept of the potential field migration, which provides fast imaging of the subsurface target (Zhdanov, 2002, 2015; Zhdanov et al. 2010, 2011). This paper develops a method of joint migration of the surface and borehole gravity data. The method is illustrated by the joint migration of the borehole and surface data for a set of the representative density models.

Migration of the surface gravity and gravity tensor fields and 3D density imaging

It is well known that the gravity field can be expressed by the gravity potential $U(\mathbf{r})$ as follows: $\boldsymbol{g}(\mathbf{r}) = \nabla U(\mathbf{r})$. The second spatial derivatives of the gravity potential $U(\mathbf{r})$,

$$\boldsymbol{g}_{\alpha\beta}(\mathbf{r}) = \frac{\partial^2}{\partial\alpha\partial\beta} U(\mathbf{r}), \quad \alpha, \beta = x, y, z$$

form a symmetric *gravity tensor*:

$$\hat{\boldsymbol{g}} = \begin{bmatrix} g_{xx} & g_{xy} & g_{xz} \\ g_{yx} & g_{yy} & g_{yz} \\ g_{zx} & g_{yy} & g_{zz} \end{bmatrix},$$

Let us assume that we have observed some component of the surface gravity field $\boldsymbol{g}_\alpha^S(\mathbf{r})$ and/or some surface gravity gradients $\boldsymbol{g}_{\alpha\beta}^S(\mathbf{r})$ over an observational surface *S*, located in the air or on the ground. The problem is to determine the 3D density distribution, $\boldsymbol{\rho}(\mathbf{r}')$, under the ground.

The surface migration gravity field, $\boldsymbol{g}_\alpha^{Sm}(\mathbf{r})$, is introduced as a result of application of the adjoint gravity operator, $\boldsymbol{A}_\alpha^{S*}$, to the observed component of the surface gravity field $\boldsymbol{g}_\alpha^S(\mathbf{r})$:

$$\boldsymbol{g}_\alpha^{Sm}(\mathbf{r}) = \boldsymbol{A}_\alpha^{S*} \boldsymbol{g}_\alpha^S \tag{1}$$

where the adjoint operator $\boldsymbol{A}_\alpha^{S*}$ for the gravity problem is equal to:

$$\boldsymbol{A}_{\alpha}^{S*}(f) = \iint_S \frac{f(\mathbf{r})}{|\mathbf{r}'-\mathbf{r}|^3} K_\alpha(\mathbf{r}'-\mathbf{r}) ds, \quad (2)$$

where the kernels are equal to $K_\alpha(\mathbf{r}'-\mathbf{r}) = \alpha' - \alpha$, $\alpha = x, y, z$.

From the physical point of view, the migration field is obtained by moving the sources of the observed gravity field above the observational surface. Nevertheless, the migration field contains some remnant information about the original sources of the gravity anomaly. That is why it can be used in imaging the sources of the gravity field.

In a similar way, we can introduce a surface migration gravity tensor field $\boldsymbol{g}_{\alpha\beta}^{Sm}(\mathbf{r})$ and use the following notations for the components of this tensor field:

$$\boldsymbol{g}_{\alpha\beta}^{Sm}(\mathbf{r}) = \boldsymbol{A}_{\alpha\beta}^{S*} \boldsymbol{g}_{\alpha\beta}^{S}, \quad (3)$$

where the adjoint operators, $\boldsymbol{A}_{\alpha\beta}^{S*}$, applied to some function $f(\mathbf{r})$, are given by the formulas:

$$\boldsymbol{A}_{\alpha\beta}^{S*}(f) = \iint_S \frac{f(\mathbf{r})}{|\mathbf{r}'-\mathbf{r}|^3} K_{\alpha\beta}(\mathbf{r}'-\mathbf{r}) ds, \quad (4)$$

where the kernels, $K_{\alpha\beta}$ are equal to

$$K_{\alpha\beta}(\boldsymbol{r}'-\boldsymbol{r}) = \begin{cases} 3\frac{(\alpha-\alpha\prime)(\beta-\beta\prime)}{|\mathbf{r}'-\mathbf{r}|^2}, & \alpha \neq \beta \\ 3\frac{(\alpha-\alpha\prime)}{|\mathbf{r}'-\mathbf{r}|^2} - 1, & \alpha = \beta \end{cases}, \alpha, \beta = x, y, z.$$

We should note, however, that the direct migration of the observed gravity and/or gravity tensor fields does not produce an adequate image of the subsurface density distribution because the migration fields rapidly attenuate with the depth, as one can see from expressions (2) and (4). In order to image the sources of the gravity fields at their correct location, one should apply an appropriate spatial weighting operator to the migration fields. This weighting operator is constructed based on the integrated sensitivity of the data to the density.

We can find a distribution of the density of the gravity field sources, described by the following expression:

$$\boldsymbol{\rho}_{\alpha}^{Sm}(\mathbf{r}) = k_\alpha^S \left(\boldsymbol{w}_\alpha^S(z)\right)^{-2} \boldsymbol{g}_\alpha^{Sm}, \quad (5)$$

where $\boldsymbol{\rho}_{\alpha}^{Sm}$ is called a *migration density*.

The unknown coefficient k_α can be determined by a linear line search (Zhdanov, 2002; 2015) according to the following:

$$k_\alpha^S = \frac{\|\boldsymbol{A}_\alpha^{w*}\boldsymbol{g}_\alpha^S\|_M^2}{\|\boldsymbol{A}_\alpha^{w}\boldsymbol{A}_\alpha^{w*}\boldsymbol{g}_\alpha^S\|_D^2}, \quad \boldsymbol{A}_\alpha^{w} = \boldsymbol{A}_\alpha^{S}\boldsymbol{W}_\alpha^{-1},$$

and the linear weighting operator $\boldsymbol{W}_m = \boldsymbol{W}_\alpha$ is selected as a linear operator of multiplication of the density $\boldsymbol{\rho}$ by a function, w_α; equal to the square root of the integrated sensitivity of the gravity field, $\boldsymbol{S}_\alpha$.

In a similar way, we can introduce a migration density based on the gravity tensor migration:

$$\boldsymbol{\rho}_{\alpha\beta}^{Sm}(\mathbf{r}) = k_{\alpha\beta}^S \left(\boldsymbol{w}_{\alpha\beta}^S(z)\right)^{-2} \boldsymbol{g}_{\alpha\beta}^{Sm}, \quad (6)$$

where:

$$k_{\alpha\beta}^S = \frac{\left\|\boldsymbol{A}_{\alpha\beta}^{w*}\boldsymbol{g}_{\alpha\beta}^S\right\|_M^2}{\left\|\boldsymbol{A}_{\alpha\beta}^{w}\boldsymbol{A}_{\alpha\beta}^{w*}\boldsymbol{g}_{\alpha\beta}^S\right\|_D^2}$$

Functions $\boldsymbol{w}_{\alpha\beta}^S$ are equal to the square root of the integrated sensitivity of the gravity tensor fields, $\boldsymbol{S}_{\alpha\beta}^S$, respectively.

A *tensor field migration density*, defined by expression (6) is proportional to the magnitude of the weighted tensor migration field $\boldsymbol{g}_{\alpha\beta}^{Sm}$. Thus, migration transformation provides a stable algorithm for calculating migration density.

Migration of the borehole gravity and gravity tensor fields and 3D density imaging

Let us assume that we have observed some component of the borehole gravity field $\boldsymbol{g}_\alpha^B(\mathbf{r})$ and/or some borehole gravity gradients $\boldsymbol{g}_{\alpha\beta}^S(\mathbf{r})$ along an observational line L, associated with a given borehole. The problem is to determine the 3D density distribution, $\boldsymbol{\rho}(\mathbf{r}')$, around the borehole. Following Liu and Zhdanov (2011), the borehole *migration gravity field*, $\boldsymbol{g}_\alpha^{Bm}(\mathbf{r})$, is introduced as a result of application of the adjoint gravity operator, $\boldsymbol{A}_\alpha^{B*}$ to the observed gravity field:

$$\boldsymbol{g}_\alpha^{Bm}(\mathbf{r}) = \boldsymbol{A}_\alpha^{B*}\boldsymbol{g}_\alpha^B \quad (7)$$

where the adjoint operator $\boldsymbol{A}_\alpha^{B*}$ for the borehole gravity problem is equal:

$$\boldsymbol{A}_\alpha^{B*}(f) = \int_L \frac{f(\mathbf{r})}{|\mathbf{r}'-\mathbf{r}|^3} K_\alpha(\mathbf{r}'-\mathbf{r}) dl, \quad (8)$$

In a similar way, we can introduce a migration field, $\boldsymbol{g}_{\alpha\beta}^{Bm}(\mathbf{r})$, of the borehole gravity tensor components observed along a borehole L, and use the following notations for the components of this tensor field:

$$\boldsymbol{g}_{\alpha\beta}^{Bm}(\mathbf{r}) = \boldsymbol{A}_{\alpha\beta}^{B*}\boldsymbol{g}_{\alpha\beta}^B \quad (9)$$

where the corresponding adjoint operators, $\boldsymbol{A}_{\alpha\beta}^{B*}$, applied to some function $f(\mathbf{r})$, are given by:

$$\boldsymbol{A}_{\alpha\beta}^{B*}(f) = \int_L \frac{f(\mathbf{r})}{|\mathbf{r}'-\mathbf{r}|^3} K_{\alpha\beta}(\mathbf{r}'-\mathbf{r}) dl, \quad (10)$$

Thus, we can see that the migration field can be calculated everywhere around the borehole for a given values of the gravity and/or gravity gradient field, measured along the borehole. We should note, however, that the direct migration of the observed gravity and/or gravity tensor fields does not produce an adequate image of the subsurface density distribution, because the migration fields rapidly attenuate away from the borehole, as one can see from expressions (8) and (10). In order to image the sources of the gravity field at the correct location, one should apply the appropriate spatial weighting operator to the migration field. This weighting operator is constructed based on the integrated sensitivity of the gravity data to the density. Taking into account equation (9) and the direction of the steepest ascent, one can find an approximation to the distribution of the density as follows:

$$\boldsymbol{\rho}_{\alpha}^{Bm}(\mathbf{r}) = k_{\alpha}^{B}\left(\boldsymbol{w}_{\alpha}^{B}(R)\right)^{-2}\boldsymbol{g}_{\alpha}^{Bm}, \tag{11}$$

where unknown coefficient k_{α}^{B} is determined by a linear line search (Zhdanov, 2002, 2015) as follows:

$$k_{\alpha}^{B} = \frac{\left\|\boldsymbol{A}_{\alpha}^{w*}\boldsymbol{g}_{\alpha}^{S}\right\|_{M}^{2}}{\left\|\boldsymbol{A}_{\alpha}^{w}\boldsymbol{A}_{\alpha}^{w*}\boldsymbol{g}_{\alpha}^{S}\right\|_{D}^{2}}, \quad \boldsymbol{A}_{\alpha}^{w} = \boldsymbol{A}_{\alpha}^{B}\boldsymbol{W}_{\alpha}^{-1},$$

and the linear weighting operator $\boldsymbol{W}_{\alpha}$ is selected as a linear operator of multiplication of the density by a function, w_{α}^{B}, equal to the square root of the integrated sensitivity of the complex intensity of the gravity field, $\boldsymbol{S}_{\alpha}^{B}$. In a similar manner, we can introduce a migration density based on the gravity tensor migration.

Joint migration

Our goal is to jointly migrate the surface and borehole gravity fields to make a clear image of a deep target. We consider a joint migration of the multiple components of the surface and borehole gravity and gravity tensor fields according to the following formula:

$$\boldsymbol{\rho}^{m}(\mathbf{r}) = c_{\alpha}^{S}\boldsymbol{\rho}_{\alpha}^{S}(\mathbf{r}) + \sum c_{\alpha\beta}^{S}\boldsymbol{\rho}_{\alpha\beta}^{S}(\mathbf{r}) + c_{\alpha}^{B}\boldsymbol{\rho}_{\alpha}^{B}(\mathbf{r}) + \sum c_{\alpha\beta}^{B}\boldsymbol{\rho}_{\alpha\beta}^{B}(\mathbf{r}) \tag{12}$$

where c_{α}^{S}, $c_{\alpha\beta}^{S}$, c_{α}^{B}, and $c_{\alpha\beta}^{B}$ can be treated as the weights of the corresponding migration fields in the density model, which can be empirically determined from the results of the model studies.

Iterative migration

Equation (12) can produce a migration image of the density distribution in the lower half-space. A better quality migration image can be produced by repeating the migration process iteratively (Wan and Zhdanov, 2013). We begin with the migration of the gravity and/or gravity tensor field data observed on the surface and/or in the borehole. In order to check the accuracy of our migration imaging, we apply the forward modeling and compute a residual between the observed and predicted data for the given density model.

$$\boldsymbol{r}_1 = \boldsymbol{g}^{pre} - \boldsymbol{g}^{obs} \tag{13}$$

where $\boldsymbol{g}^{obs}$ is the observed gravity or gravity gradient component; $\boldsymbol{g}^{pre}$ is the predicted gravity or gravity gradient component calculated with the density $\boldsymbol{\rho}_1^{m}$ obtain from equation (12). If the residual is smaller than the prescribed accuracy level, we use the migration image as a final density model. In a case where the residual is not small enough, we migrate the residual field and produce the density correction, $\delta\boldsymbol{\rho}_1^{m}$, to the original density model using the same analysis, which we have applied for the original migration:

$$\delta\boldsymbol{\rho}_1^{m} = k\boldsymbol{w}^{-2}\boldsymbol{r}_1, \qquad \boldsymbol{\rho}_2^{m} = \boldsymbol{\rho}_1^{m} - \delta\boldsymbol{\rho}_1^{m} \tag{14}$$

where $\delta\boldsymbol{\rho}_1^{m}$ stands for the migration image obtained by residual field migration, equation (12).

A general scheme of the iterative migration can be described by the following formula:

$$\boldsymbol{\rho}_{n+1}^{m} = \boldsymbol{\rho}_{n}^{m} - \delta\boldsymbol{\rho}_{n}^{m} \tag{15}$$

The iterative migration is terminated when the residual field becomes smaller than the required accuracy level of the data fitting. The iterative migration can be combined with the regularization method. This also allows us to apply the smooth or focusing stabilizers to produce a more focused image of the target (Wan and Zhdanov, 2013).

Model study

In this section we present an example of 3D joint migration for surface and borehole gravity gradient field data. We consider a model that contains two HC reservoirs with the size of 3000 m x 1500 m x 100 m (L x W x H). It is known that the density of sandstone is between 2.2~2.8 g/cm³, the density of shale is between 2.4~2.8 g/cm³, the density of petroleum is 0.64 g/cm³, the density of seawater is about 1.02 g/cm³. Therefore we can set the anomalous density of reservoir at -1 g/cm³. The upper reservoir is located at a depth of 1 km below the surface, and the lower one is located at a depth of 2 km to the surface with a slightly large size (see Figure 1).

The synthetic observed data were computed in the set of receivers, located on the ground over an area having 7 km in the *x* direction and 5.5 km in the *y* direction with 100 m separation in both the *x* and *y* directions. A borehole is located at a point with the coordinates *x*=3300 m and *y*=3800 m. The borehole receivers are located with a vertical separation of 50 m. The observed data were contaminated by 5% random noise (see Figures 2 and 3).

For comparison, we first ran the iterative migration using the surface g_{zz} component only. The misfit reached a 5% data error level. Figure 4 shows the result of iterative migration of the surface g_{zz} component only at the cross section of *x*=3400 m.

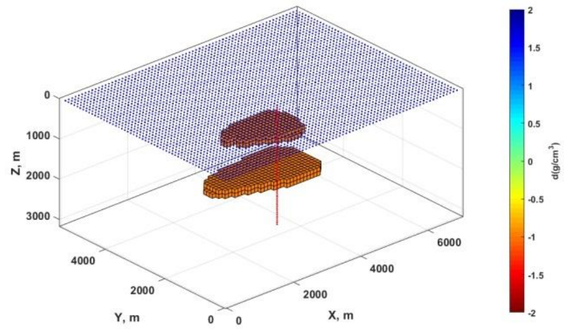

Figure 1: Model. The blue dots shows the observed station at the surface. The red dots shows the observed position in the borehole.

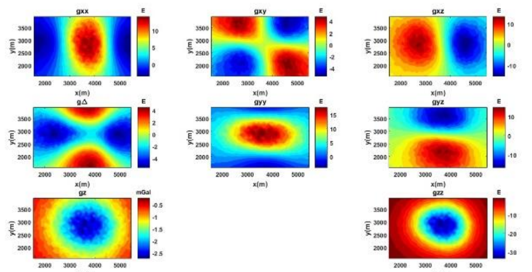

Figure 2: Maps of the observed gravity and gravity gradient data on the surface.

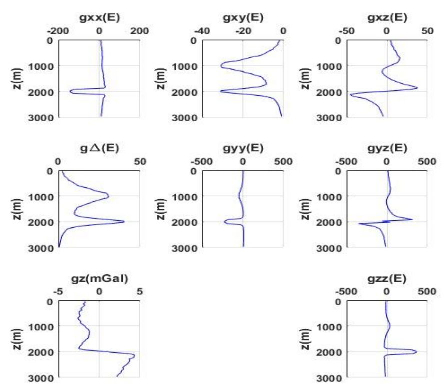

Figure 3: Profiles of the observed gravity and gravity gradient data in the borehole.

The density image shows only one target, and the lower anomalous body cannot be seen at all from the surface data migration; even the data fitting is very good and the migration only runs 5 iterations. Figure 5 shows the result from iterative migration of surface g_{zz} and borehole g_{zz} components jointly at the cross section of *x*=3400 m and *y*=2100 m. One can see that the image shows clearly the two anomalous bodies from the cross section image. The predicted data fits well the observed data in both surface and borehole data.

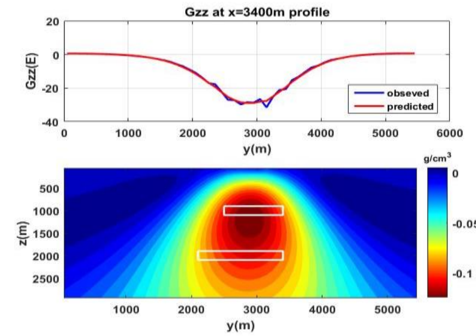

Figure 4: The result of the iterative migration of the surface g_{zz} component only at the vertical section at *x*=3400 m (the bottom panel). The blue line shows the observed data and the red line presents the predicted data on the surface (top panel).

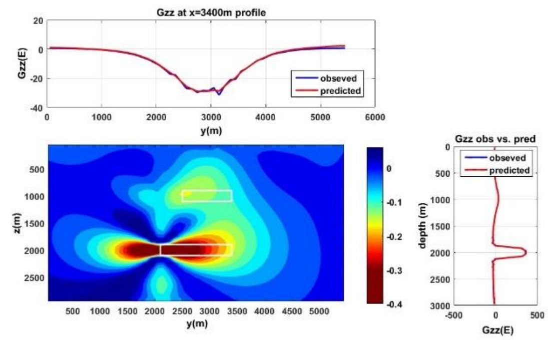

Figure 5: The result of the joint iterative migration of the surface, g_{zz}, and borehole, g_{zz}, components at the vertical section at *x*=3400 m (bottom panel). The blue lines show the observed data and the red lines present the predicted data on the surface (top panel) and in the borehole (right panel). The white lines outline the true contours of the HC reservoirs.

Conclusions

We have developed a novel approach to the joint interpretation of the surface and borehole gravity and gravity gradient data based on the concept of potential field migration. The results of the numerical model study demonstrated that the potential field migration can be used for 3D imaging of deep seated HC reservoirs. The joint migration of the surface and borehole gravity and gravity gradient components can significantly improve the imaging of 3D targets in comparison to the use of the surface data only.

Acknowledgments

The authors acknowledge the support of the University of Utah Consortium for Electromagnetic Modeling and Inversion (CEMI) and TechnoImaging for support of this research.

EDITED REFERENCES

Note: This reference list is a copyedited version of the reference list submitted by the author. Reference lists for the 2016 SEG Technical Program Expanded Abstracts have been copyedited so that references provided with the online metadata for each paper will achieve a high degree of linking to cited sources that appear on the Web.

REFERENCES

Cao, D., 2013, Impedance joint inversion of surface and borehole seismic data: GeoConvention 2013, Integration: Geoscience Engineering Partnership, AAPG Search and Discovery Article #90187.

Difrancesco, D., 2007, Advances and challenges in the development and deployment of gravity gradiometer systems: EGM 2007 International Workshop, Innovation in EM, Grav and Mag Methods: A New Perspective for Exploration.

Golden, H., W. McRae, and A. Veryaskin, 2007, Description of and results from a novel borehole gravity gradiometer: Presented at the ASEG 19th Geophysical Conference and Exhibition, http://dx.doi.org/10.1071/ASEG2007ab047.

Krahenbuhl, R., and Y. Li, 2008, Joint inversion of surface and borehole 4D gravity data for continuous characterization of fluid contact movement: 78th Annual International Meeting, SEG, Expanded Abstracts, 726–729, http://dx.doi.org/10.1190/1.3063750.

Li, Y., and D. W. Oldenburg, 2000, Joint inversion of surface and three-component borehole magnetic data: Geophysics, **65**, 540–552, http://dx.doi.org/10.1190/1.1444749.

Liu, X., and M. Zhdanov, 2011, 3D imaging of gravity gradiometry data from a single borehole using potential field migration: 81st Annual International Meeting, SEG.

McCulloh, T. H., G. R. Kandle, and J. E. Schoellhamer, 1968, Application of gravity measurements in wells to problems of reservoir evaluation: Society of Professional Well Log Analysts 9th Annual Logging Symposium Transactions, 1–29.

Nind, C., H. O. Seigel, M. Chouteau, and B. Giroux, 2007, Development of a borehole gravimeter for mining applications: First Break, **25**, 71–77.

Nind, C. J. M., and J. D. MacQueen, 2013, The borehole gravity meter: Development and results: 10th Biennial International Conference and Exposition, http://dx.doi.org/10.2118/166833-MS.

Rim, H., and Y. Li, 2010, Single-borehole imaging using gravity gradiometer data: 80th Annual International Meeting, SEG, Expanded Abstracts, 1137–1140, http://dx.doi.org/10.1190/1.3513045.

Smith, N. J., 1950, The case for gravity data from boreholes: Geophysics, **15**, 605–636, http://dx.doi.org/10.1190/1.1437623.

Sun, J., and Y. Li, 2010, Inversion of surface and borehole gravity with thresholding and density constraints, 80th Annual International Meeting, SEG, http://dx.doi.org/10.1190/1.3513191.

Wan, L., and M. S. Zhdanov, 2008, Focusing inversion of marine full-tensor gradiometry data in offshore geophysical exploration: 76th Annual International Meeting, SEG, Expanded Abstracts, 751–754, http://dx.doi.org/10.1190/1.3063755.

Wan, L., and M. Zhdanov, 2013, Iterative migration of gravity and gravity gradiometry data: 83rd Annual International Meeting, SEG, http://dx.doi.org/10.1190/segam2013-1036.1.

Zhdanov, M. S., 2002, Geophysical inverse theory and regularization problems: Elsevier.

Zhdanov, M. S., 2015, Inverse theory and applications in geophysics: Elsevier.

Zhdanov, M. S., X. Liu, and G. Wilson, 2010, Potential field migration for rapid 3D imaging of gravity gradiometry surveys: First Break, **28**, 47–51.

Zhdanov, M. S., X. Liu, G. A. Wilson, and L. Wan, 2011, Potential field migration for rapid imaging of gravity gradiometry data: Geophysical Prospecting, **59**, 1052–1071, http://dx.doi.org/10.1111/j.1365-2478.2011.01005.x.